Available online at www.sciencedirect.com
SCIENCE DIRECT®
Journal of Molecular Graphics and Modelling 24 (2006) 456–464
Journal of Molecular Graphics and Modelling
www.elsevier.com/locate/JMGM

Three-dimensional models of histamine H_3 receptor antagonist complexes and their pharmacophore

Frank U. Axe [a], Scott D. Bembenek [b,*], Sándor Szalma [c]

[a] *Axe Consulting Services, 14595 Surrey Junction Lane, Sutter Creek, CA 95685, USA*
[b] *Johnson & Johnson Pharmaceutical Research and Development, 3210 Merryfield Row, San Diego, CA 92121, USA*
[c] *MeTa Informatics, 12987 Caminito Bautizo, San Diego, CA 92130, USA*

Accepted 3 October 2005
Available online 28 December 2005

Abstract

Molecular modeling was used to analyze the binding mode and activities of histamine H_3 receptor antagonists. A model of the H_3 receptor was constructed through homology modeling methods based on the crystal structure of bovine rhodopsin. Known H_3 antagonists were interactively docked into the putative antagonist binding pocket and the resultant model was subjected to molecular mechanics energy minimization and molecular dynamics simulations which included a continuum model of the lipid bilayer and intra- and extracellular aqueous environments surrounding the transmembrane helices. The transmemebrane helices stayed well embedded in the dielectric slab representing the lipid bilayer and the intra- and extracellular loops remain situated in the aqueous solvent region of the model during molecular dynamics simulations of up to 200 ps in duration. A pharmacophore model was calculated by mapping the features common to three active compounds three-dimensionally in space. The 3D pharmacophore model complements our atomistic receptor/ligand modeling. The H_3 antagonist pharmacophore consists of two protonation sites (i.e. basic centers) connected by a central aromatic ring or hydrophobic region. These two basic sites can simultaneously interact with Asp 114 (3.32) in helix III and a Glu 206 (5.46) in helix V which are believed to be the key residues that histamine interacts with to stabilize the receptor in the active state. The interaction with Glu 206 is consistent with the enhanced activity resulting from the additional basic site. In addition to these two salt bridging interactions, the central region of these antagonists contains a lipophilic group, usually an aromatic ring, that is found to interact with several nearby hydrophobic side chains. The picture of antagonist binding provided by these models is consistent with earlier pharmacophore models for H_3 antagonists with some exceptions.
© 2005 Elsevier Inc. All rights reserved.

Keywords: Histamine H_3 receptor; Binding mode; Homology model; Pharmacophore; Molecular dynamics and generalized Born model

1. Introduction

Histamine is a potent biogenic amine that elicits a variety of physiological effects, which are played out by one of four known histamine receptors (H_1, H_2, H_3, and H_4) [1–5]. These physiological effects include allergic reactions (H_1), gastric acid secretion (H_2), mediation of neurotransmitter release (H_3) and immunological response (H_4). Both the H_1 and H_2 receptors are well known and effective antagonists have been developed to control a range of maladies, including allergies and gastric ulcers, and constitute some of the most commercially successful drugs on the market today [6,7]. The H_3 and H_4 receptors have been discovered fairly recently and their biological significance as well as antagonists that modulate them are an active area of investigation by industry and academia [8,9].

The H_3 receptor is found in the central and peripheral nervous system on the presynaptic cleft of neurons where it functions as a negative regulator of histamine as well as mediates the release of other neurotransmitters [10,11]. Possible roles for an antagonist of this target include treatments for narcolepsy, arousal, ADHD, cognition, and memory disorders [12,13]. The H_3 receptor belongs to the G-coupled protein receptor (GPCR) super family containing a transmembrane region consisting of a seven alpha-helical bundle. This transmembrane region is often the site of ligand and drug interaction [14,15]. This is particularly true for the aminoergic receptors which include histamine, dopamine, serotonin and andrenergic receptors [14,15]. For each of these receptors the natural ligand is derived from an amino acid and contains a primary amine that is believed to interact with a highly

* Corresponding author. Tel.: +1 8583203375; fax: +1 8587843058.
E-mail addresses: frankaxe@aol.com (F.U. Axe), sbembene@prdus.jnj.com (S.D. Bembenek).

1093-3263/$ – see front matter © 2005 Elsevier Inc. All rights reserved.
doi:10.1016/j.jmgm.2005.10.005

conserved aspartic acid side-chain in the third helix inside the helical bundle [14,15]. The same is true for many of their antagonists [14,15].

Several groups have reported the discovery of potent and selective non-imidazole H_3 receptor antagonists [16–20]. In general these compounds differ from H_1, H_2 and even H_4 receptor antagonists in their chemical structures and features, and the general H_3 pharmacophore has been described [17]. Specifically the non-imidazole based antagonists contain at least one basic amine as do most antagonists of aminoergic receptors, but in many instances a second basic site is present which significantly enhances activity. And these two basic centers are linked by a lipophilic group [17]. Several examples of H_3 antagonists illustrating the features of this pharmacophore [16–18] are shown in Fig. 1. In each of these examples there is a primary basic group, either a piperidine or pyrolidine, which is connected by an alkyl linkage. In each chemical series there is an example of an antagonist with a second basic group. In each of the three cases presented in Fig. 1 (**1** and **2**, **3** and **4**, **5** and **6**) the addition of the secondary basic group increases the binding affinity by 100-, 10- and 8-fold, respectively. Each of these chemical series also contains at least one lipophilic aromatic ring.

Three-dimensional atomistic models of antagonist-receptor complexes have been used to investigate the details of ligand and drug interactions with GPCRs and have been successful in providing important insights regarding their binding [21–24]. These models are usually based on a homology model built from the X-ray structure of bovine rhodopsin [25], but several first principle approaches to building the receptor model are being used as well [26]. Docking of the ligand is performed by automated or manual docking using either site directed mutagenesis data and/or sequence homology knowledge as to where the molecule binds. Usually the ligand is energy minimized in the binding region with some or complete relaxation of the receptor model but it is rare to perform lengthy dynamics since this requires a representation of the lipid bilayer and the surrounding aqueous environment, which is very costly to include in the dynamics calculations. Although there are a number of studies which include explicit bilayer and solvent using a periodic boundary condition they are in general the exception in modeling GPCR ligand interactions [14,26]. Recently, continuum dielectric models, based on the Born approximation, have been extended to handle the unique situation of membrane bound proteins [27,28]. These implicit membrane models were successfully applied to the study of the dynamics of a small helical peptide at a aqueous/lipid interface and the static orientation of bovine and bacterial rhodopsin crystal structures in their native bilayer environment [27,28]. However, no full relaxation or molecular dynamics of a GPCR structure using this novel implicit membrane model have been reported to date.

Pharmacophore modeling can provide a qualitative picture of ligand receptor binding by identifying the important features for binding and their spatial arrangements [29]. This approach has been particularly successful for investigating GPCR/ligand binding modes and is complementary to 3D receptor/ligand modelling [30]. Consequently, two papers describing pharmacophore models of H_3 receptor antagonists have been published [31,32]. In both studies only imidazole based antagonists were considered. To date no quantitative pharmacophore models based on non-imidazole antagonist compounds have been reported.

We present a computational study of the binding of several H_3 antagonists to the H_3 receptor using a homology model for the receptor and employing this novel continuum dielectric model for the surrounding bilayer environment. This work represents the first use of this continuum method in which complete relaxation and molecular dynamics were run with the ligands bound to a GPCR. We examine the utility of the implicit membrane model to study GPCR drug interactions. We use sequence analysis and the results of existing site directed mutagenesis studies on the closely related histamine H_1, H_2 and H_4 receptors, which were used to define the internal site of agonism and antagonism of known ligands and drugs, to define the putative antagonist binding site in our model. We then used this information to dock and simulate known H_3 antagonist compounds bound to the receptor model. In addition we

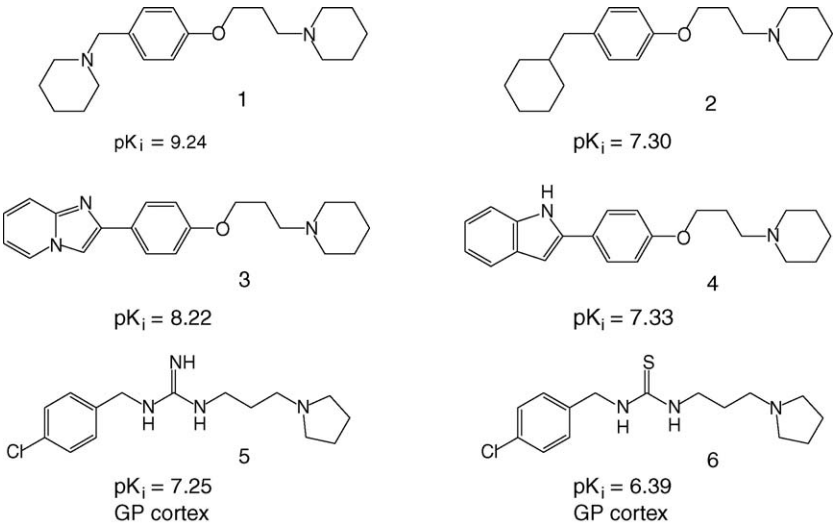

Fig. 1. Non-imidazole H_3 antagonists reported in the literature illustrating the SAR.

developed a pharmacophore model by three-dimensional alignment of the common features of several active compounds. We use the resulting models to investigate ligand binding in the H_3 receptor and the nature of the two basic and the lipophilic features of the H_3 phamacophore model and compare and contrast their similarities and differences.

2. Methods

2.1. Sequence alignment and homology modeling

The transmembrane portion of the H_3 receptor was built by homology modeling techniques based on the 2.8 Å

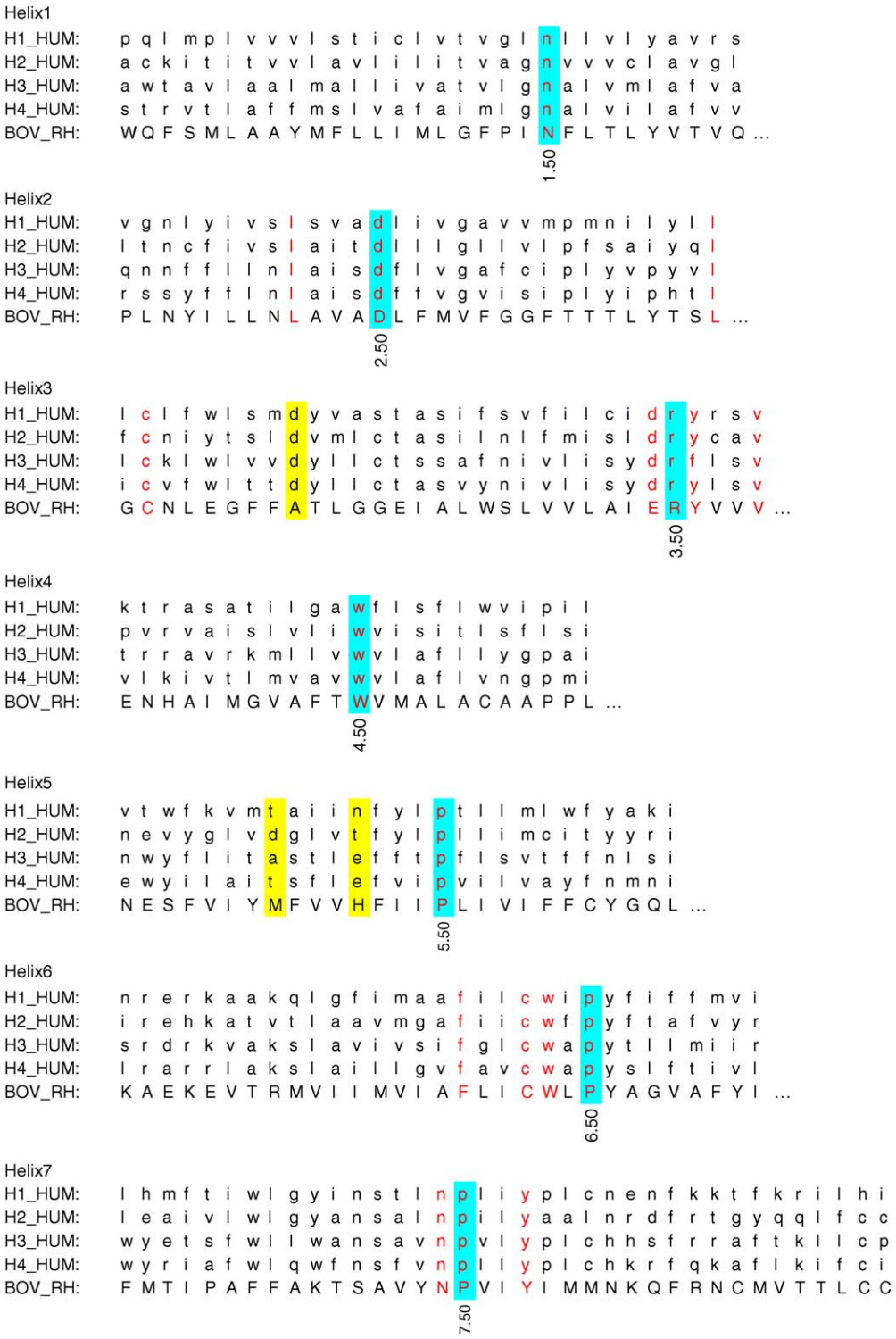

Fig. 2. Alignment of the human H_1, H_2, H_3 and H_4 receptor sequences with bovine rhodopsin. Highly conserved residues are highlighted in red. Residues highlighted in cyan are the *x*.50 (where *x* is the helix number) residues of the Ballesteros and Weinstein index system (ref. [33]). The key residues involved in agonist and antagonist binding in helices III and V and highlighted in yellow.

resolution crystal structure of Bovine Rhodopsin [25] (pdb entry 1F88) which is the most accurate rhodopsin structure available. The primary sequence of the H_3 receptor was aligned with bovine rhodopsin based upon highly conserved amino acid residues in the seven helices. All homology models were constructed with the MODELER program [33,34]. Seven of the eight extra- and intra-cellular loops were modeled directly from the rhodopsin structure. The intra-cellular loop between helices V and VI is very long and most likely adopts a folded structure that is not represented by the rhodopsin structure, and so it was truncated by including 10 residues leading out of helix V and the 10 residues leading into helix VI.

Our alignment of the human H_3 sequence to the bovine rhodopsin sequence included all four human histamine receptor sequences and the sequences of several other aminoergic receptors including several subtypes of the dopamine, serotonin and andrenergic receptors. We used the Clustal W program [35] to provide the locations of the transmembrane helices and an initial alignment of the sequences, but ultimately we relied upon the identification of key motifs and highly conserved residues within the sequences to complete the alignment (i.e. the ''DRY'' motif at the end of helix III). This sequence alignment is shown in Fig. 2. This alignment was also confirmed by predicting the helical regions with the hidden Markov model method TMHMM [36]. We use the absolute residue number as well as the relative numbering scheme of Ballesteros and Weinstein [37] to designate specific amino acids throughout the text.

2.2. Atomistic modeling methods

All molecular mechanics minimization and molecular dynamics (MD) calculations were performed with the CHARMm program [38,39]. A united atom force field, which includes explicit polar hydrogens, was used (CHARMPLR). Forcefield parameters were assigned to each ligand molecule atom based on its closest description in the CHARMm forcefield [38]. Each basic nitrogen included an explicit hydrogen. Partial atomic charges were assigned by using the default charging scheme in InsightII for the CHARMPLR forcefield resulting in a formal positive charge around each protonation site.

The lipid bilayer was represented by the generalized Born-solvent accessible surface area implicit membrane (GBSA/IM) model of Spassov et al. [27] This is a continuum dielectric model based on the original generalized Born model [40]. In this model the aqueous solvent comprises a high dielectric region and the lipid membrane and the interior of the membrane bound protein taken together comprise a low dielectric region (Fig. 3). The value of the dielectric constant for the membrane interior (ε_m) was set to 2, while the value of the dielectric constant for the aqueous solvent regions surrounding the bilayer (ε_{solv}) was set to 80. In our simulations the bilayer had a width of 30 Å. The initial orientation of the GPCR antagonist model with respect to the continuum bilayer was optimized via

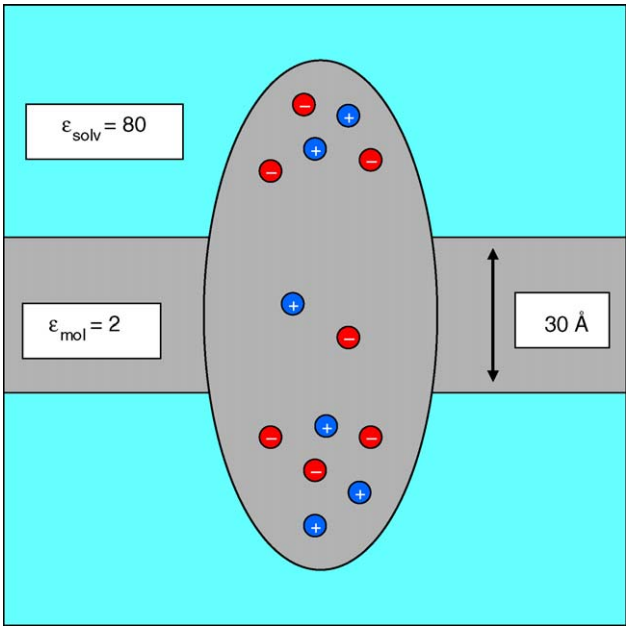

Fig. 3. A schematic representation of the continuum dielectric regions for a GPCR embedded in a lipid bilayer, which is used in the generalized Born solvent accessible surface area implicit membrane model. The solvent region is colored cyan and the membrane slab and transmembrane regions are colored grey.

a rigid body procedure that systematically rotated and translated the complex to determine the optimal position [27].

The optimally oriented structure was then energy minimized with 1000 steps of steepest descents followed by 3000 steps of adopted basis Newton Raphson minimization. The MD calculations employed a Verlet method [41] to integrate the equations of motion using a time step of 0.001 picoseconds (ps). The MD calculations consisted of three stages. An initial heating phase in which the temperature was increased from 0 K to the target temperature of 300 K over the course of 4000 time steps. This was followed by an equilibration phase of 40,000 time steps. Finally, production runs consisting of stages of 100 ps in duration were run and the trajectory was sampled every 50 steps. The temperature was maintained by using the Berendsen temperature bath method [42]. The Shake algorithm was applied to all hydrogens during the dynamics [43].

2.3. Pharmacophore modeling

All pharmacophore modeling was carried out with the Catalyst program using the Hip-Hop option [44]. This is a procedure that takes 3D conformations for each training molecule identifies common features and overlays them in space [29]. We used the automatic conformer generation feature employing the flexible option. We used three active molecules to define the pharmacophore, which are compounds **1**, **7**, and **8** (Fig. 4). We felt that these compounds capture all of the features required for activity while providing significant structural variation as well.

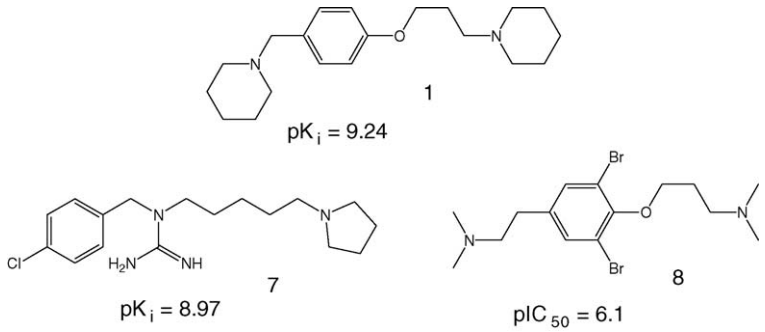

Fig. 4. H_3 antagonist molecules reported in the literature used to build the pharmacophore model.

3. Results and discussion

3.1. Agonist/antagonist binding site

The putative agonist and antagonist binding sites of the H_1, H_2 and H_4 receptors have been investigated by site directed mutagenesis [45–48]. A study on the H_1 receptor found [45] that the Asp 107 (3.32) in helix III and Thr 194 (5.42) and Asn 198 (5.46) in helix V are important for histamine binding, while only Asp 107 was important for antagonist binding. The antagonist used is this study was mepyramine, a classic H_1 antagonist with two aromatic rings and a basic amine arrayed in a triangular constellation. In another study [46] on the H_1 receptor an antagonist that possessed a carboxylic acid group on one of the aromatic rings was found to interact with a Lys 191 (5.39) in helix V. In the same study several hydrophobic residues in helices IV and VI were found to be important too. All of the residues found to be important for antagonist binding are in the histamine binding site. In a study on the H_2 receptor the Asp 98 (3.32) in helix III and Asp 186 (5.42) in helix V were important for both agonist and antagonist binding [47]. In the same study Thr 190 (5.46) was also shown to play a minor role in ligand binding as well. The antagonist used in this study was [methyl-3H]tiotidine, which has two guanidinium groups that can potentially interact with these two acidic residues (Asp 98 and Asp 186). Finally, a study on the H_4 receptor revealed that Asp 94 (3.32) in helix III and Glu 182 (5.46) in helix V are important for histamine binding [48].

These mutagenesis studies provide the basis for rationalizing where the binding site for our H_3 antagonists is, namely in the region between Asp 114 (3.32) in helix III and Glu 206 (5.46) in helix V. This is a reasonable assumption in light of the experimental evidence on the closely related histamine receptors and that the same region is the experimentally confirmed site of antagonist binding in several related biogenic amine receptors as well [14]. We manually docked our ligands into this putative antagonist binding site using interactive graphics. This involved placing the protonated sites on the molecule near Asp 114 (3.32) and Glu 206 (5.46) while minimizing any bad contacts.

3.2. Membrane model

Our H_3 ligand receptor complexes were simulated with the CHARMm program in the presence of the GBSA/IM model. The optimal position of the receptor complex in the 30 Å dielectric slab was optimized by performing a rigid body rotation and translation systematic search [27]. This initial optimization placed the helices in the membrane slab with the intra- and extracellular loops in the solvent regions. The orientation of the helical axes was roughly in the direction of the normal to the solvent/membrane interface. This model was then energy minimized and subjected to a molecular dynamics heating and equilibration protocol before 200 ps of production simulation was run and sampled. The helices of the receptor model remained embedded in the lipid membrane slab while the intra- and extracellular loops remained in the aqueous solvent region throughout the course of the simulation indicating that the model provided a reasonable description of the bilayer environment. The orientation of the H_3 receptor relative to the membrane slab is shown in Fig. 5, which is the final configuration from a 200 ps trajectory of the H_3 receptor complexed with compound **1**. We did notice some minor ''unraveling'' of the transmembrane helices as the molecular dynamics progressed but the helical structure was maintained. This may be the result of the lack of an exact structure for the inter-helical loops and the truncation of the loop region

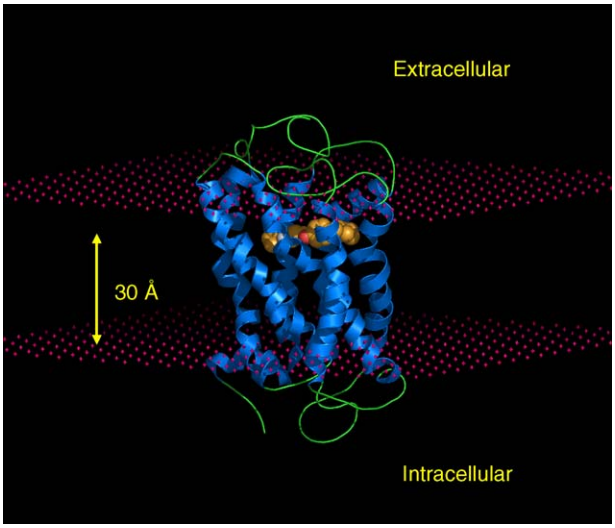

Fig. 5. The H_3 receptor model with compound **1** bound after heating equilibration and 200 ps of molecular dynamics. The red hatches represent the location of the membrane slab region in our GBIM model, which is 30 Å in width.

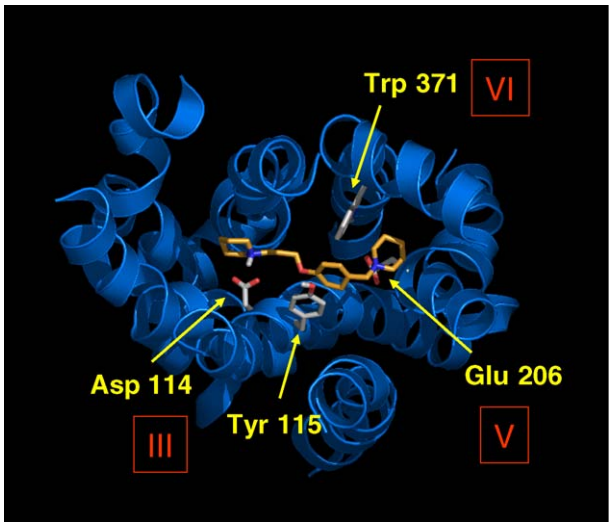

Fig. 6. H_3 receptor model with compound **1** bound in the putative binding site showing the interaction with several key amino acid residue side chains in the helical bundle interior.

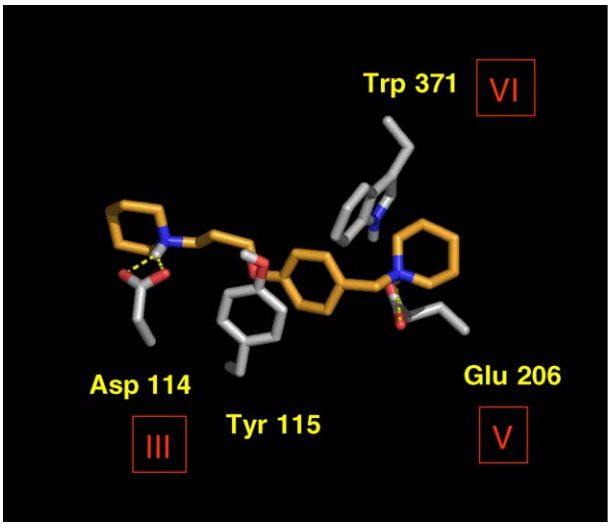

Fig. 7. A detailed view of the interactions between compound **1** and the key amino acid side chains of the putative H_3 antagonist binding site.

spanning helices V and VI. Knowing this we felt confident that fully relaxing our homology model was reasonable.

3.3. Ligand binding interactions

Two of the literature compounds (**1** and **7**) were analyzed in our current model. Compound **1** was docked, equilibrated and simulated for 200 ps. Fig. 6 shows the final configuration of compound **1** bound to the H_3 receptor from the end of a 200 ps MD simulation. In Fig. 6, we are looking down from the extracellular region into the interior of the seven helical bundle where compound **1** is seen to be interacting with Asp 114 (3.32) and Glu 206 (5.46). The aromatic ring in compound **1** is seen to be interacting with the aromatic ring of Tyr 115 in a stacking mode. The same aromatic ring in compound **1** also is in close contact with the aromatic ring of Trp 371, forming a roughly 90° dihedral angle between the two rings. A close up of all of these interactions are shown in Fig. 7. These interactions were all analyzed quantitatively in detail and the results of this analysis is reported in Fig. 8. A plot of the distance between the proton on the nitrogen of the propyl-piperidine ring and the oxygens of the carboxylate of Asp 114 is shown in Fig. 8A for the last 100 ps of the MD trajectory. The distance ranges between 1.68 and 2.84 Å and the average distance is calculated

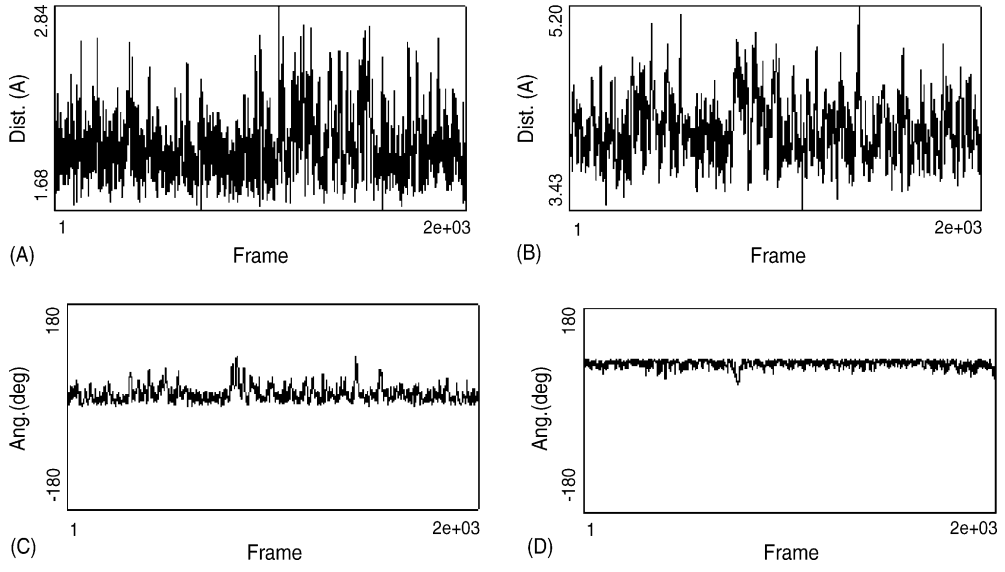

Fig. 8. (A) Plot of the distance between the proton of the nitrogen of the propyl-piperidine of compound **1** and the carboxylate oxygens of Asp 114 for the final 100 ps of the MD trajectory. The average distance is 2.05 Å. (B) Plot of the distance between the centroid of the aromatic ring of compound **1** and the centroid of the aromatic ring of Tyr 115 for the final 100 ps of the MD trajectory. The average distance is 4.14 Å. (C) Plot of the dihedral angle between the aromatic ring of compound **1** the aromatic ring of Tyr 115 for the final 100 ps of the MD trajectory. The average angle is 23°. (D) Plot of the dihedral angle between the aromatic ring of compound **1** the aromatic ring of Trp 371 for the final 100 ps of the MD trajectory. The average angle is 82°.

to be 2.05 Å. A similar set of results was found for the distance between the proton of the benzyl-piperidine group and the oxygens of Glu 206 with a distance of 2.18 Å. Fig. 8B shows a plot of the distance between the centroid of the aromatic ring in compound **1** and the centroid of the aromatic ring in Tyr 115. It ranges in value from 3.43 to 5.20 Å with an average of 4.14 Å. Fig. 8C shows a plot of the dihedral angle between the plane of the aromatic ring in compound **1** and the plane of the aromatic ring in Tyr 115. It ranges between 0 and 90° with an average value of 23°. Fig. 8D shows a plot of the dihedral angle between the plane of the aromatic ring in compound **1** and the aromatic ring of Trp 371. It ranges between 45 and 90° with an average value of 82°.

Analysis of the MD trajectory of compound **1** bound to the H_3 receptor model reveals that the two basic nitrogens interact strongly with the carboxylates of Asp 114 and Glu 206. These interactions are well maintained through the course of the heating and equilibration and over 200 ps of MD simulation. The fluctuations in the propyl-piperidine proton oxygen distances fall into a very narrow range further indicating the strong interactions of these two salt bridging interactions. The aromatic group of compound **1** forms a fairly stable pi-stacking van der Waals interaction with the aromatic group of Tyr 115, which was well maintained during the course of the MD simulation. The fluctuation in the non-bonded distance and the ring-ring dihedral angle are consistent with a stable stacking interaction of these two aromatic rings. The close proximity of Asp 114 to Tyr 115, which is relatively fixed since they are on the same helix, allows this stacking interaction to take place only at the precise distance afforded by the propylene linker length. Apodaca et al. noted a 15- to 40-fold reduction in activity when the propylene linker in **1** was shortened to an ethylene linker [17].

In a similar fashion we modeled compound **7** bound to the H_3 receptor model. A configuration from the end of a 100 ps MD simulation is shown in Fig. 9. The interactions that occur between Asp 114 and Glu 206 are expected. The guanidinium group forms a bidentate interaction with the carboxylate group of Glu 206 with an average carboxylate oxygen-HN distance of 2.20 Å. The pyrolidine Asp 114 interaction is very similar to the analogous piperidine interaction in compound **1** with an average oxygen-HN distance of 2.07 Å. However, the binding mode of compound **7** differs from that of compound **1** in that the pentylene linkage appears to make the hydrophobic contact with Tyr 115 and the terminal aromatic ring interacts more exclusively with Trp 371, since it is not capable of being in the same location as the aromatic ring in **1**. The differences in the binding modes of compounds **1** and **7** are indicative of the structural differences of these two molecules and the plasticity of the ligand binding site.

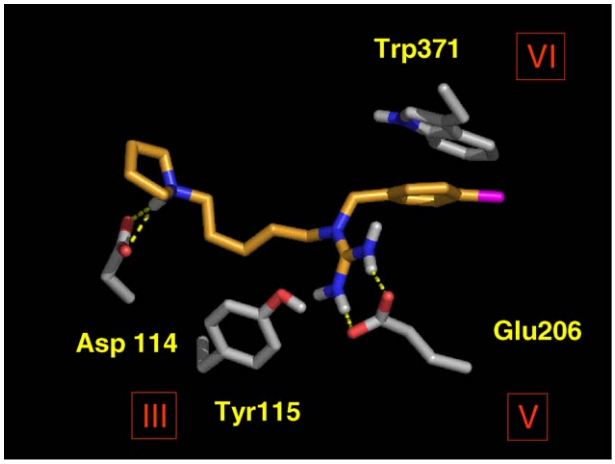

Fig. 9. A detailed view of the interactions between compound **7** and the key amino acid side chains of the putative H_3 antagonist binding site.

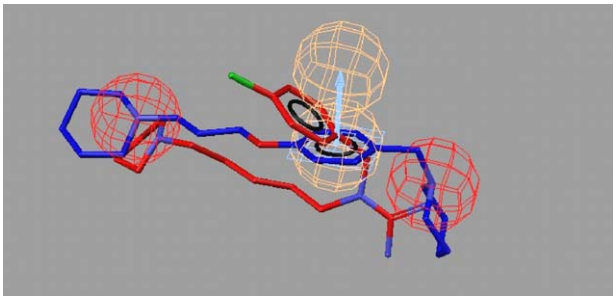

Fig. 10. Calculated pharmacophore model with compounds **1** (blue) and **7** (red) aligned to the features (positive ionic – red spheres, aromatic – tan sphere).

3.4. Pharmacophore model

The calculated pharmacophore model with compounds **1** and **7** overlayed is shown in Fig. 10. This pharmacophore model consists of three features, two positive ionic centers and an aromatic ring, which is very similar to what was proposed by Apadoca et al. previously [17]. The three features in compounds **1** and **7** align well with the elements of the pharmacophore. The aromatic ring of compound **7** in the pharmacophore model is in the general location of the aromatic ring in compound **1**, which is in contrast to the relative positions of the same rings in the two MD simulations. This qualitative difference between the two types of models may be a limitation of the pharmacophore model because of its propensity to align common features. Other pharmacophore models were built using different training sets of molecules and similar results were obtained [49].

4. Conclusions

We have used three-dimensional atomistic modeling to explore the putative antagonist binding site in the histamine H_3 receptor. Starting with a homology model for the H_3 receptor we used molecular mechanics and dynamics in conjunction with a novel continuum dielectric model that accounts for the aqueous solvent and lipid bilayer regions. This was the first time this novel continuum dielectric model was applied to the study of GPCR antagonist binding. This implicit membrane model has several advantages over other approaches in that one may fully relax the GPCR complex in the presence of a realistic representation of the lipid bilayer and surrounding solvent but without the costly computational overhead of an explicit bilayer

and solvent in a periodic boundary condition. We used sequence alignments and site directed mutagenesis information on the three related histamine receptor sub-types to postulate the location of the antagonist binding site. We docked our ligands into this putative binding site manually and ran lengthy MD simulations. We predict that the two basic features found in more potent H_3 antagonists interact with the highly conserved Asp 114 (3.32) in helix III and Glu 206 (5.46) in helix V. The central aromatic feature present in many of the H_3 antagonists makes van der Waals contact with several nearby hydrophobic aromatic residue side chains including Tyr 115 (3.33) and Trp 371 (6.48). All of these interactions were well maintained throughout the course of our simulations. The longer aliphatic chain of **7** can also provide the same hydrophobic contact with Tyr 115 that the aromatic ring of **1** does. Our results are consistent with the general pharmacophore model [17] of Apadoca et al. All four of the above mentioned residues would be of primary importance in any future site directed mutagenesis study probing the H_3 binding site. We also think it would be interesting to see the role of varying the length of the Glu 206 side chain by mutating it to an Asp. We can exploit this unique binding mode to create highly potent and selective H_3 receptor antagonists. This study validates the utility of implicit membrane method to the study of GPCR ligand interactions for the purpose of drug discovery.

References

[1] S.J. Hill, C.R. Ganellin, H. Timmerman, J.C. Schwartz, N.P. Shankley, J.M. Young, W. Schunack, R. Levi, H.L. Hass, International union of pharmacology. XIII. Classification of histamine receptors, Pharmacol. Rev. 49 (1997) 253–278.

[2] L.B. Hough, Genomics meets histamine receptors: new subtypes, new receptors, Mol. Pharmacol. 59 (2001) 415–419.

[3] J.C. Schwartz, H.L. Haas, The Histamine Receptor, Wiley, Liss, New York, 1992.

[4] J. Ring, Histamine and allergic diseases, in: New Trends in Allergy, Springer-Verlag Press, Berlin, 1985, pp. 44–77.

[5] S.J. Hill, Distribution, properties and functional characteristics of three classes of histamine receptor, Pharmacol. Rev. 42 (1990) 45–83.

[6] M.Q. Zhang, R. Leurs, H. Timmerman, Histamine H1-receptor antagonists, in: M.E. Wolff (Ed.), Burger's Medicinal Chemistry and Drug Discovery, fifth ed., John Wiley and Sons, New York, 1997, pp. 496–559.

[7] H. van der Goot, A. Bast, H. Timmerman, Structural requirements for histamine H2 agonists and H2 antagonists, in: B. Uvnas (Ed.), Handbook of Experimental Pharmacology, Springer-Verlag, Berlin Press, 1991, pp. 573–749.

[8] T.W. Lovenberg, B.L. Roland, S.J. Wilson, X. Jiang, J. Pyati, A. Huvar, M.R. Jackson, M.G. Enlander, Cloning and functional expression of the human histamine H_3 receptor, Pharmacol. Exp. Therapeutics 55 (1999) 1101–1107.

[9] C. Liu, X.J. Ma, X. Jiang, S.J. Wilson, C.L. Hofstra, J. Blevitt, J. Pyati, X. Li, W. Chai, N. Carruthers, T.W. Lovenberg, Cloning and pharmacological characterization of a fourth histamine receptor (H_4) expressed in bone marrow, Mol. Pharmacol. 59 (2001) 420–426.

[10] H. Stark, J.M. Arrang, X. Ligneau, M. Garbarg, C.R. Ganellin, J.C. Schwartz, J.C. Schunack, The histamine H_3 receptor and its ligands, Prog. Med. Chem. 38 (2001) 279–308.

[11] E. Schlicker, M. Kathmann, Modulation of the in vitro neurotransmission in the CNS and in the retina via H_3 heteroreceptors, in: R. Leurs, H. Timmerman (Eds.), The Histamine H_3 Receptor: A Target for New Drugs, Elsevier Science B.V., Amsterdam, 1998, pp. 13–26.

[12] R. Leurs, P. Blandina, C. Tedford, H. Timmerman, Therapeutic potential of histamine H_3 receptor agonists and antagonists, Trends Pharmacol. Sci. 19 (1998) 177–183.

[13] R. Leurs, R.C. Vollinga, H. Timmerman, The medicinal chemistry and therapeutic potentials of ligands of the histamine H_3 receptor, in: E. Jucker (Ed.), Progress in Drug Research, vol. 45, Birkenhäuser Verlag, Basel, 1995, pp. 107–165.

[14] G. Müller, Towards 3D structures of G protein coupled receptors: a multidisciplinary approach, Curr. Med. Chem. 7 (2000) 861–888.

[15] W.K. Kroeze, K. Kristiansen, B.L. Roth, Molecular biology of serotonin recptors – structure and function at the molecular level, Curr. Topics Med. Chem. 2 (2002) 507–528.

[16] W. Chai, J.G. Breitenbucher, A. Kwok, X. Li, V. Wong, N.I. Carruthers, T.W. Lovenberg, C. Mazur, S.J. Wilson, F.U. Axe, T.K. Jones, Non-imidazole heterocyclic histamine H_3 receptor antagonists, Bioorg. Med. Chem. Lett. 13 (2003) 1767–1770.

[17] R. Apodaca, C.A. Dvorak, W. Xiao, A.J. Barbier, J.D. Boggs, S.J. Wilson, T.W. Lovenberg, N.I. Carruthers, A new class of diamine-based human histamine H_3 receptor antagonists 4-(aminoalkoxy)benzylamines, J. Med. Chem. 46 (2003) 3938–3944.

[18] I.D. Linney, I.M. Buck, E.A. Harper, S.B. Kalindjian, M.J. Pether, N.P. Shankley, G.F. Watt, P.T. Wright, Design, synthesis, and structure-activity relationships of novel non-imidazole histamine H_3 receptor antagonists, J. Med. Chem. 43 (2000) 2362–2370.

[19] J. Apelt, X. Ligneau, H.H. Pertz, J.M. Arrang, C.R. Ganellin, J.C. Schwartz, W. Schunack, H. Stark, Development of a new class of nonimidazole histamine H_3 receptor ligands with combined inhibitory histamine N-methyltransferase activity, J. Med. Chem. 45 (2002) 1128–1141.

[20] C. Shah, L. McAtee, J.G. Breitenbucher, D. Rudolph, X. Li, T.W. Lovenberg, C. Mazur, S.J. Wilson, N.I. Carruthers, Novel histamine H_3 receptor antagonists, Bioorg. Med. Chem. Lett. 12 (2002) 3309–3312.

[21] M.F. Hibert, Protein homology modeling and drug discovery, in: The Practice of Medicinal Chemistry, Academic Press, New York, 1996, pp. 523–546.

[22] R. Kiss, Z. Kovári, G.M. Keserű, Homology modeling and binding site mapping of the human H1 receptor, Eur. J. Med. Chem. 39 (2004) 959–967.

[23] A. Evers, T. Klabunde, Structure-based drug discovery using GPCR homology modeling: successful virtual screening for antagonists of the Alpha1A adrenergic receptor, J. Med. Chem. 48 (2004) 1088–1097.

[24] K.E. Furse, T.P. Lybrand, Three-dimensional models for β-adrenergic receptor complexes with agonists and antagonists, J. Med. Chem. 46 (2003) 4450–4462.

[25] K. Palczewski, T. Kumasaka, T. Hori, C.A. Behnke, H. Motoshima, B.A. Fox, I.L. Trong, D.C. Teller, T. Okada, R.E. Stenkamp, M. Yamamoto, M. Miyano, Crystal structure of rhodopsin: a G protein-coupled receptor, Science 289 (2000) 739–745.

[26] N. Vaidehi, W.B. Floriano, R. Trabanino, S.E. Hall, P. Freddolino, E.J. Choi, G. Zamanakos, W.A. Goddard III, Prediction of structure and function of G protein coupled receptors, PNAS 99 (2002) 12622–12627.

[27] V.Z. Spassov, L. Yan, S. Szalma, Introducing an implicit membrane in generalized Born/solvent accessibility continuum solvent models, J. Phys. Chem. B 106 (2002) 8726–8738.

[28] W. Im, M. Feig, C.L. Brooks III, An implicit membrane generalized Born theory for the study of structure, stability, and interactins of membrane proteins, Biophys. J. (2003) 2900–2918.

[29] O.O. Clement, A.T. Mehl, HipHop: pharmacophores based on multiple common-feature alignments, in: O.F. Güner (Ed.), Pharmacophore Perception, Development and Use in Drug Design, International University Line, La Jolla, CA, 2000, pp. 71–84.

[30] J. Quintana, M. Contijoch, R. Cuberes, J. Frigola, Structure-activity relationships and molecular modeling studies of a series of H1 antihistamines, in: F. Sanz, J. Giraldo, F. Manaut (Eds.), QSAR and Molecular Modeling: Concepts, Computational Tools and Biological Applications, Prous Science Publishers, Barcelona, 1995, pp. 282–288.

[31] I.J.P. de Esch, H. Timmerman, W.M.P.B. Menge, P.H.J. Nederkoorm, A qualitative model for the histamine H_3 receptor explaining agonistic and

antagonistic activity simultaneously, Arch. Pharm. Pharm. Med. Chem. 333 (2000) 254–260.
[32] I.J.P. de Esch, J.E.J. Mills, T.D.J. Perkins, G. Romeo, M. Hoffmann, K. Wieland, R. Leurs, W.M.P.B. Menge, P.H.J. Nederkoorn, P.M. Dean, H. Timmerman, Development of a pharmacophore model for histamine H_3 receptor antagonists, using the newly developed molecular modeling program SLATE, J. Med. Chem. 44 (2001) 1666–1674.
[33] A. Sali, T.L. Blundell, Comparative protein modeling by satisfaction of spatial restraints, J. Mol. Biol. 234 (1993) 779–815.
[34] MODELER, version 4, Accelrys, San Diego, CA.
[35] J.D. Thompson, D.G. Higgins, T.J. Gibson, Clustal W: improving the sensitivity of progressive multiple sequence alignment through sequence weighting, positions-specific gap penalties and weight matrix choice, Nucleic Acids Res. 22 (1994) 4673–4680.
[36] A. Krogh, B. Larsson, G. von Heijne, E.L.L. Sonnhammer, Predicting transmembrane protein topology with a hidden Markov model: application to complete genomes, J. Mol. Biol. 305 (2001) 567–580.
[37] J.A. Ballesteros, H. Weinstein, Integrated methods for the construction of three dimensional models and computational probing of structure-function relations in G-protein coupled receptors, Methods Neurosci. 25 (1995) 366–428.
[38] B.R. Brooks, R.E. Bruccoleri, B.D. Olafson, D.J. States, S. Swaminathan, M. Karplus, CHARMM: a program for macromolecular energy, minimization, and dynamics calculations, J. Compd. Chem. 4 (1983) 187–217.
[39] CHARMm, version 27b4, Accelrys, San Diego, CA.
[40] B.N. Dominy, C.L. Brooks III, Development of a generalized Born model parameterization for proteins and nucleic acids, J. Phys. Chem. B 103 (1999) 3765–3773.
[41] L. Verlet, Computer 'experiments' on classical fluids. I. Thermodynamical properties of Lennard–Jones molecules, Phys. Rev. 159 (1967) 98–103.
[42] H.J.C. Berendsen, J.P.M. Postma, W.F. van Gunsteren, A. DiNola, J.R. Haak, Molecular dynamics with coupling to an external bath, J. Chem. Phys. 81 (1984) 3684–3690.
[43] W.F. van Gunsteren, H.J.C. Berendsen, Algorithms for macromolecular dynamics and constraint dynamics, Mol. Phys. 34 (1977) 1311–1327.
[44] Catalyst, version 8.0, Accelrys, San Diego, CA.
[45] K. Ohta, H. Hayashi, H. Mizuguchi, H. Kagamiyama, K. Fujimoto, H. Fukui, Site-directed mutagenesis of the histamine H_1 receptor: roles of aspartic acid[107], asparagine[198] and threonine[194], Biochem. Biophys. Res. Commun. 203 (1994) 1096–1101.
[46] K. Wieland, A.M. Ter Laak, M.J. Smit, R. Kühne, H. Timmerman, R. Leurs, Mutational analysis of the antagonist-binding site of the histamine H_1 receptor, J. Biol. Chem. 274 (1999) 29994–30000.
[47] I. Gantz, J. DelValle, L.D. Wang, T. Tashiro, G. Munzert, Y.J. Guo, Y. Konda, T. Yamada, Molecular basis for the interation of histamine with histamine H2 receptor, J. Biol. Chem. 267 (1992) 20840–20843.
[48] N. Shin, E. Coates, N.J. Murgolo, K.L. Morse, M. Bayne, C.D. Strader, F.J. Monsma, Molecular modeling and site-specific mutagenesis of the histamine-binding site of the histamine H4 receptor, Mol. Pharmacol. 62 (2002) 38–47.
[49] F.U. Axe, Unpublished results.